Peer-reviewed version available at Chemosensors 2018, 6, 58; doi:10.3390/chemosensors6040058

Propylene glycol stabilizes the linear response of glutamate biosensor: potential implications for in-vivo neurochemical monitoring.

Gaia Rocchitta[1]*, Andrea Bacciu[1], Paola Arrigo[1], Rossana Migheli[1], Gianfranco Bazzu[1], Pier Andrea Serra[1]

1 Department of Medical, Surgical and Experimental Sciences, Sassari University, Viale San Pietro 43/b, 07100 Sassari (Italy)

*Correspondence: grocchitta@uniss.it; Tel.: +39079228526

Abstract:

L-glutamate is one the most important excitatory neurotransmitter at central nervous system level and it is implicated in several pathologies. So, it is very important to monitor its variations, in real time in animal models' brain. Amperometric biosensors have been used because of their very high temporal and spatial resolution, and because suitable for a short to mid-term implantation. The present study aimed to develop and characterize a new glutamate biosensor design that exploits the selectivity of Glutamate Oxidase (GluOx) for l-glutamate, and the capability of a small molecule as propylene glycol (PG) to influence and extend the stability and the activity of enzyme. Different designs were evaluated by modifying the main components in their concentrations to find the most suitable design. Moreover, enzyme concentrations from 100 U/ml up to 200 U/ml were verified and different PG concentrations (1%, 0.1% and 0.05%) were tested. The most suitable selected design was Pt_c/PPD/PEI(1%)$_2$/GlutOx$_5$/PG(0.1%) and it was compared to the same already described design loading PEDGE, instead of PG, in terms of over-time performances. PG has proved to be capable of determining an over-time stability of the glutamate biosensor in particular in terms of linear region slope (LRS) up to 21 days.

Keywords: L-gutamate, amperometric biosensors, propylene glycol, stability over time

1. Introduction

L-glutamate is one the most important excitatory neurotransmitter at Central nervous System (CNS) level, and it is involved not only in neurotransmission [1, 2] but also in normal brain functioning as movement, cognitive processes, memory and plasticity [3]. So, it has become a very important compound not only in biomedical analysis but also for the implications in the field of food [4].

L-glutamate has been also demonstrated to be involved in many pathologies as epilepsy, schizophrenia, stroke and neurological disorders as Parkinson's disease [5-7] but also amyotrophic lateral sclerosis and Alzheimer's disease [8, 9]. For these reasons, it has become very important to measure glutamate concentrations, and their variations, in real time in animal models.

The most widely used technique for in vivo glutamate monitoring was undoubtedly microdialysis [10-14] but electrochemical biosensors have been used for many years because of the minimal invasiveness, the rapid and real-time quantification of the studied analytes [15-17].

In addition to the previous characteristics, the biosensors, in particular in case of glutamate, require a high sensitivity in monitoring because of the glutamate low concentrations detected in the brain, assessed being in the range of 1–10 μM, and that can be dependent on the brain region of implantation [1].

One of the open challenges in biosensing is, without a doubt, the real-time glutamate monitoring in CNS in the presence of high levels of electrochemical interferents. Actually, the specificity of amperometric biosensors can be affected by interfering compounds is present in high concentration as in case for ascorbic acid (AA) at CNS level [18, 19]. This is the case that occurs during the monitoring of glutamate that is found, in physiological conditions, at rather low concentrations [1].

So, because their very high temporal and spatial resolution, implantable amperometric biosensors have proved to be suitable for the implantation, from short to mid-term period, in brain tissues of animal models.

Amperometric biosensors exploit the capability of the biocomponent, usually represented by an enzyme, to specifically bind the studied analyte [17, 20] and to generate some electroactive compound, converting a biological signal into a measurable electrical signal [21].

In this work, a biosensor design has been developed and characterized for the detection of glutamate, exploiting the capability of L-glutamate oxidase (GluOx) enzyme to convert L-glutamate as follows:

$$\text{L-Glutamate} + H_2O + \text{GluOx/FAD} \longrightarrow \alpha\text{-ketoglutarate} + NH_3 + \text{GluOx/FADH}_2 \quad (1)$$

$$\text{GluOx/FADH}_2 + O_2 \longrightarrow \text{GluOx/FAD} + H_2O_2 \quad (2)$$

$$H_2O_2 \longrightarrow O_2 + 2H^+ + 2e^- \quad (3)$$

The hydrogen peroxide (H_2O_2), produced by the enzymatic reaction, can be easily amperometrically measured at a Pt surface by applying a high fixed anodic potential of +0.7 V vs Ag/AgCl [22-24].

In the past, it has been highlighted that the presence of an enzymatic stabilizer as polyethileneimine (PEI) is of fundamental importance for increasing the analytical performances of glutamate biosensor [1, 23, 25]. In this work, the impact of the use of PEI it will be also evaluated.

Moreover, this work will be focused on the entrapment strategies needed to block all the layered biosensor components in order to ameliorate over-time performances of glutamate biosensor, both for an eventual acute and mid-term implant.

In the past, lots of approaches have been adopted to entrap enzyme molecules on the biosensor transducer surface such as covalent coupling, physical adsorption, gel entrapment or crosslinking [17, 26].

About crosslinking strategy, the most commonly used for the immobilization of enzymes are polymeric films deposited on top of layered components [27-31] or glutaraldehyde crosslink [32-35]. Poly-(ethylene glycol) diglycidyl ether (PEGDE) as crosslinking agent has been proposed in the past [4] and also recently it has been used, resulting a more suitable crosslinker compared with glutaraldehyde for the immobilization of glutamate oxidase and capable to determine better biosensor sensitivities [1, 35-37]. It has been demonstrated the epoxide groups present in PEGDE molecule can interact with amino groups allowing the cross-linking with the enzyme and also the covalent bonding of the enzyme layer to the surface [38].

In the past, some papers demonstrated that some compounds as amino acids, methylamines, sugars and polyols, among them propylene glycol, could act as protein stabilizers because of the hydrophobic interaction with protein molecules and because of the protection of enzyme activity [39-43]. Among all polyols, in the present paper special attention has been given to propylene glycol (PG) that is a nontoxic compound commonly used in the pharmaceutical products as a solvent or stabilizer for many compounds. In the present study it has been evaluated the role of propylene glycol as enzyme stabilizer and containment network of the layered components constituting the biosensors and its impact on kinetic and analytical parameters but also on the stability overtime of the proposed glutamate biosensor design. Propylene glycol biosensors design has been then compared to equivalent but with PEGDE.

2. Materials and Methods

2.1. Chemicals and Reagents

All chemical compounds were bought from Sigma-Aldrich and used as supplied.

The phosphate-buffered saline (PBS, 50 mM) solution used for calibrations and electropolymerisations was made using 0.15 M NaCl, 0.05 M NaH_2PO_4 and 0.04 M NaOH, and adjusted to pH 7.4.

Sodium glutamate (Glut, 1 M and 10 mM), PG, PEGDE (0.1%), polyethyleneimmine (PEI, 1%) solutions were diluted in bidistilled water, while o-phenylenediamine (OPD) was prepared in fresh PBS. Stock solutions of ascorbic acid (AA, 100 mM) were prepared in HCL 0.01 N and stored at -20 °C.

Glutamate Oxidase (GluOx, Streptomyces sp., EC 1.4.3.11, 200 U/ml) was from Yamasa Corp.

Teflon insulated Platinum/Iridium wire (Pt, 90:10, Ø = 125 µm) was bought from Advent Research Materials (Eynsham, UK).

2.2. Instrumentation and software

For all electrochemical experiments, a conventional three-electrode cell was used which consisted of a beaker holding 20 ml of fresh PBS, four glutamate biosensors as working electrodes, an Ag/AgCl (3M) electrode (Bioanalytical Systems, Inc. West Lafayette, USA) and a large surface stainless steel needle as auxiliary electrode. A four-channel potentiostat (eDAQ Quadstat, e-Corder 410, eDAQ Europe, Poland) was utilized for all electrochemical procedures. All potentials used in this work refer to the aforementioned reference electrode.

2.2 Biosensor construction and characterisation

As shown in Figure 1, different biosensor designs were developed, all of them based on a cylindrical geometry (1 mm length and 125 µm diameter).

Biosensors were manufactured as previously described [1, 23, 24] and realizing different strategies differentiating biosensor designs, varying components concentrations and processes, to obtain the most performing.

Briefly, a 3 cm portion of Pt wire was cut and from one edge, 3 mm of insulation was eliminated in order to allow bare metal to be welded to its support. From the other edge of the wire, a 1 mm of bare metal was exposed for modifications.

First, on Day 0, PPD electropolymerisation was carried out by immersing the Pt wires in an OPD 300 mM solution freshly prepared in PBS, and by applying a positive potential of +0.7 V vs Ag/AgCl (3M) for 30 minutes.

After having rinsed electrodes in pure water, they were immersed twice in a PEI 1 % solution, waiting 5 minutes between each immersion. Then, electrodes were dipped 5 times in the GlutOx solution, at different concentrations (dependently on the chosen design), allowing 5 minutes from one dip and another to allow the drying of each enzyme layer. On top, a layer of PG, at different concentrations, (dependently on the chosen design), or PEGDE, was deposited by a single dip, allowing the layer to dry for 30 minutes. At the end of procedures, biosensors were immersed in fresh PBS and a positive potential of +0.7 V vs Ag/AgCl was applied to allow an overnight stabilisation of the currents.

On Day 1 a full glutamate calibration, ranging between 0 and 100 mM, was carried out in fresh PBS by the addition of known volumes of the Glut stock solutions (1 M and 10 mM). On same day an AA calibration ranging from 0 to 1000 µM was performed to assess the design capability to block currents

from interfering compounds. For all designs, the same calibrations' protocol was repeated on Day 7, and for some of them appropriately selected, also at Day 10, 15 and 21 to assess biosensor ageing. Different designs have been manufactured (Figure 1): the basic design (D1) involved the deposition of all the components previously described except the PEI. A second design (D2) was made by the deposition of all components and above all PG (0.1%). Starting from D2 design, some variations on GluOx and PG concentrations were performed and characterized. A third design (D3) was built by depositing above all layered components PEGDE (0.1%). Biosensor performances were evaluated from calibration data in terms of enzymatic kinetic (V_{MAX} and K_M) and analytical performances (linear region slope - LRS, AA blocking).

All designs were tested for currents due to the main interfering compounds as DA, DOPAC, UA, 5-HIAA. In all cases, the above-mentioned compounds did not determine any interfering signal on biosensor glutamate monitoring, as previously showed [44].

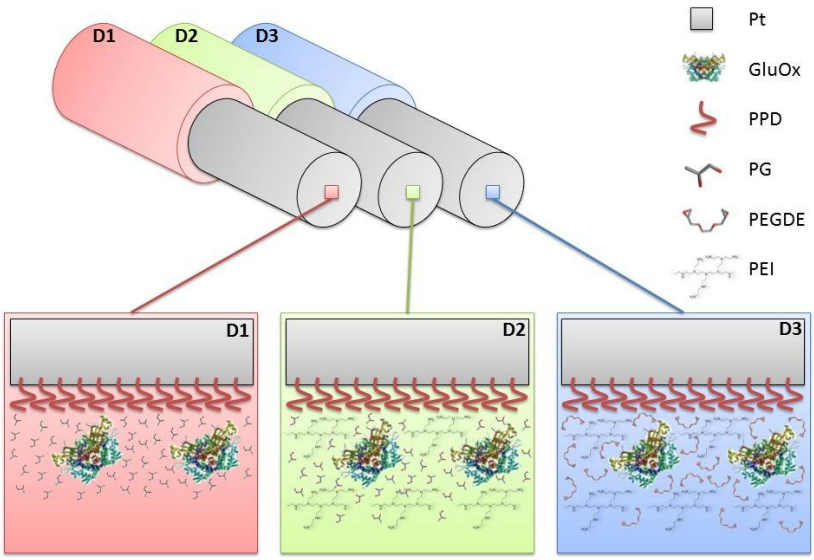

Figure 1: Schematic representation of the main designs of glutamate biosensors characterized in this study. **D1**: Pt_c/PPD/GluOx5/PG (0.1%); **D2**: Ptc/PPD/PEI(1%)$_2$/GluOx$_5$/PG(0.1%); **D3**: Pt_c/PPD/PEI(1%)/GluOx$_5$/PEGDE(0.1%). Pt_c: Pt cylinder 1 mm long, 125 µm diameter; GluOx: L-glutamate oxidase; PPD: poly-ortho-phenylenediamine; PEI: polyethyleneimine; PG: propylene glycol; PEGDE: Poly(ethylene glycol) diglycidyl ether. The subscript number represents the number of dip−evaporation deposition steps and in brackets the concentration of the component.

2.3 Statistical analysis

After calibrations, biosensor currents were plotted versus Glut and AA concentrations. First, for glutamate data a nonlinear fitting with Michaelis–Menten equation was performed on the entire

concentration range (0–100 mM) to evaluate V_{MAX} and apparent K_M. Linear regressions (slope) were calculated at low concentrations (0–0.6 mM). Recorded currents were given in nanoamperes (nA) and expressed as baseline-subtracted values ± standard error of the mean.

AA shielding was evaluated by taking in account the current recorded at 500 µM and ΔI value, which stands for the difference between the current resulting from the injection of 1000 µM and 500 µM of AA in the electrochemical cell, as discussed previously [45].

Statistical significance (P values) between groups was assessed using unpaired t-tests by GraphPad Prism 5.02 v software.

3. Results and discussion

3.1 In Vitro performances of glutamate biosensors

As shown in Figure 2 and Table 1, three different glutamate biosensors design were compared. We opted to compare responses to Glu, in terms of kinetic parameters (V_{MAX} and K_M) analytical parameters (LRS) and AA for different biosensor designs (n = 4 for each group): We also decide to evaluate the above-mentioned parameters at Day 1 (Panel A) and Day 7 (Panel B): LRS are showed in their respective insets.

The D1 design (red curve) produced the worst performances, if compared with D2 and D3 designs. In fact, it showed, at Day 1, a V_{MAX}= 52.71 ± 1.70 nA, a K_M= 1275.02 ± 163.81 µM (R^2=0.996) and a LRS= 0.030 ± 0.001 nA/ µM (inset, Panel A), while the response to AA 500 µM was 1,484 ± 0,056 nA and the ΔI was -0.027 nA. This design performances, ad Day 7, further worsened. In fact, it displayed a V_{MAX}= 36.23 ± 1.67 nA, a K_M= 1717.12 ± 299.12 µM (R^2=0.997) and a LRS= 0.020 ± 0.001 nA/µM, while the response to AA 500 µM was 26.07 ± 12.18 nA and the ΔI was 15.10 nA. From these results, it is evident that the presence of PEI in the biosensor design is fundamental in order to increase the enzymatic activity and make the biosensor more performing, as previously demonstrated [23, 25]. In fact, the polycation PEI has been demonstrated to be able to stabilize different enzymes because of the reduction of the repulsion between anionic charges on GluOx molecules, determining a better biosensor efficiency [23, 25].

The D2 design showed at Day 1 a V_{MAX}= 335.91 ± 5.03 nA, a K_M= 524.53 ± 37.62 µM (R^2=0.999) and a LRS= 0.318 ± 0.011 nA/ µM; the response to AA 500 µM was 1.250 ± 0.124 nA while the ΔI was 0.482 nA. At Day 7, the same design, displayed a V_{MAX}= 392.16 ± 7.73 nA, a K_M= 892.8 ± 73.55 µM (R^2=0.989), and a LRS= 0.288 ± 0.008 nA/ µM; the response to AA 500 µM was 2.153 ± 0.430 nA while the ΔI was 1.061 nA.

This design held, in general, acceptable kinetic performances over time. In fact, in this design albeit K_M increased of 70.21%, the V_{MAX} augmented of 16.75% and LRS suffered a slight reduction (-9.5%). Conversely, AA shielding suffered a sustained worsening (+48.5%).

These results seem to highlight an increase of active enzyme molecules on the biosensor surface from Day 1 to Day 7, while the K_M suffered of a increase and LRS a slight decrease. Even the shielding for AA underwent a worsening, pointing out that, although the performances have remained sufficiently good over time, an improvement in shielding towards interfering molecules is required.

The D3 design (blue curve) demonstrated, at Day 1, a V_{MAX}= 409.73 ± 5.58 nA, a K_M= 620.23 ± 37.65 µM (R^2=0.995) and a LRS= 0.352 ± 0.014 nA/µM and the response to AA 500 µM was 0,867 ± 0,074 nA and the ΔI was 0.388 nA. This design, if compared with D1 design, proved to be the most performing on Day 1, because of higher V_{MAX} and LRS, but also for a lower K_M. Even the shielding capability of AA resulted being better. At Day 7, the same design, displayed a V_{MAX}= 399.5 ± 4.88 nA, a KM= 680.34 ± 34.85 µM (R^2=0.996), and a LRS= 0.330 ± 0.011 nA/ µM; the response to AA 500 µM was 4.127± 1,103 nA while the ΔI was 1.848 nA.

Therefore, at Day 7, it occurred a decrease in V_{MAX} (-2.5%) and AA shielding (+76 % of AA current) and LRS (about -8%) and an increase in K_M (+9.7%), demonstrating a general over-time worsening if compared with D2 design.

The crosslinker PEGDE has been largely used in biosensor fabrications and in particular for glutamate biosensors [1, 35-37]. Our results, in the considered range of time, confirm the capability of PEGDE to avoid the loss of substrate specificity, that can occur during enzyme immobilization. This phenomenon is due to its mild action towards the enzyme molecules, due to its epoxy moiety on enzyme amino groups, thus saving enzyme conformation [37].

Preprints (www.preprints.org) | NOT PEER-REVIEWED | Posted: 26 October 2018 doi:10.20944/preprints201810.0630.v1

Peer-reviewed version available at Chemosensors 2018, 6, 58; doi:10.3390/chemosensors6040058

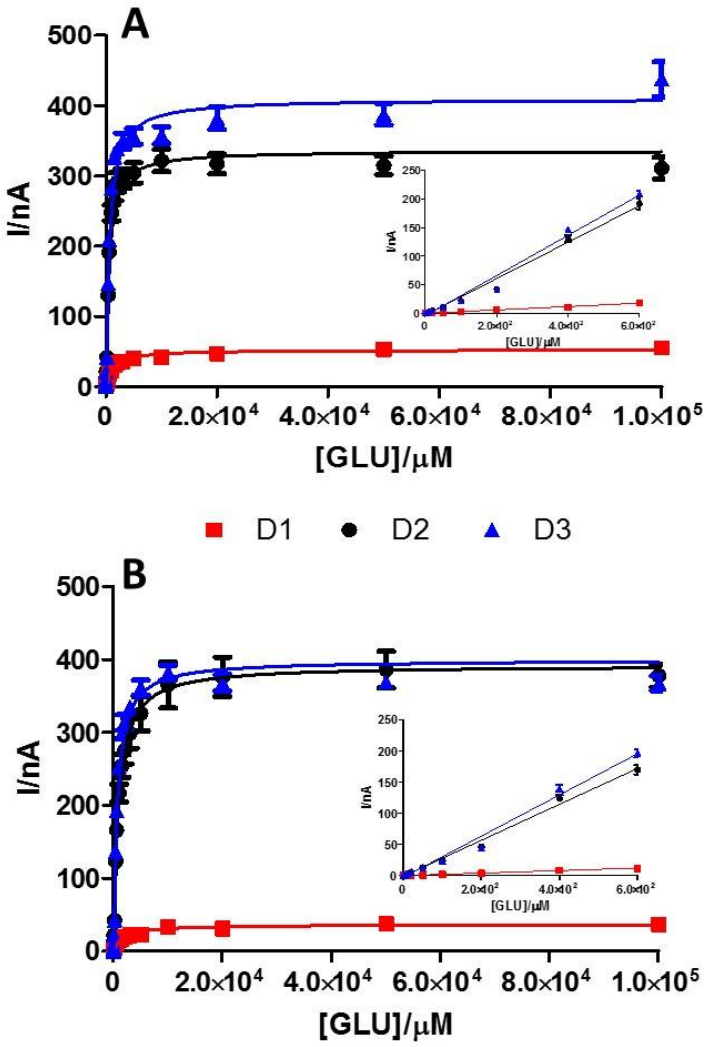

Figure 2: Michaelis-Menten kinetics plots of glutamate calibrations on different biosensor designs at Day 1 (panel A) and Day 7 (panel B), ranging from 0 to 100 mM. In the insets the relative 0-0.6 mM linear regressions. **D1**: red curve; **D2**: black curve; **D3**: blue curve.

PARAMETERS	D1	D2	D3
DAY 1			
V_{MAX} (nA)	52.71 ± 1.70	335.91 ± 5.03	409.73 ± 5.58
K_M [µM]	1275.02 ± 163.81	524.53 ± 37.62	620.23 ± 37.65
LRS (nA/µM)	0.030 ± 0.001	0.318 ± 0.011	0.352 ± 0.014
I_{lim} (nA)	1.984 ± 0,056	1.450 ± 0.124	0.867 ± 0.074
ΔI	-0.027	0.482	0.388
DAY 7			
V_{MAX} (nA)	36.23 ± 1.67	392.16 ± 7.73	399.5 ± 4.88
K_M [µM]	1717.12 ± 299.12	892.8 ± 73.55	680.34 ± 34.85
LRS (nA/µM)	0.020 ± 0.001	0.288 ± 0.008	0.330 ± 0.011
I_{lim}(nA)	26.072 ± 12.178	2.153 ± 0.430	4.127± 1.103
ΔI	15.103	1.061	1.848

Table 1. In vitro characterization of three different biosensor designs at Day 1 and day 7 in terms of Michaelis–Menten kinetic parameters (V_{MAX} and K_M) and analytical parameters (Linear Region Slope -LRS) for each design. **D1**: Pt_c/PPD/GluOx5/PG (0.1%); **D2**: Ptc/PPD/PEI(1%)$_2$/GluOx$_5$/PG(0.1%); **D3**: Pt_c/PPD/PEI(1%)/GluOx$_5$/PEGDE(0.1%). Pt_c: Pt cylinder 1 mm long, 125 µm diameter; GluOx: L-glutamate oxidase; PPD: poly-ortho-phenylenediamine; PEI: polyethyleneimine; PG: propylene glycol; PEGDE: Poly(ethylene glycol) diglycidyl ether. The subscript number represents the number of dip−evaporation deposition steps and in brackets the concentration of the component.

3.2 Effects of the difference of enzyme concentration in glutamate biosensor parameters

In the present study different concentrations of enzyme were used. As displayed in Figure 3, at Day 1 (Panel A) the concentration of 100 U/ml (red curve), if compared with 200 U/ml design (black curve), determined a decrease in V_{MAX} and an increase in K_M, that were equal to 98.19 ± 7.67 nA and 1088.03 ± 348.90 µM (R^2=0.997), proving that this design possessed fewer active enzyme molecules on the surface and their accessibility resulted difficult for the substrate, while the LRS was 0.068 ± 0.003 nA/µM. This design showed a current equal to 1.79 ± 0.18 nA at 500 µM of AA and a ΔI= 1.60 nA. At Day 7 (Panel B, red curve), it occurred a general improvement in biosensor performances. In fact, the above-mentioned design showed a V_{MAX}= 111.02 ± 5.74 nA, a K_M= 819.65 ± 184.34 µM (R^2=0.994), and a LRS= 0,077 ± 0,004 nA/µM. The AA shielding worsened, in fact AA at 500 µM it was 11.31 ± 3.634 nA and ΔI= 7.398 nA.

By increasing the concentration of the enzyme up to 150 U/ml (blue curve) the observed parameters at Day 1 were 232.81 ± 5.65 nA and 508.54 ± 59.54 µM (R^2=0.997) and 0.237 ± 0.002 nA/µM for V_{MAX}, K_M and LRS respectively. The AA shielding resulted similar to that obtained for the design loading 100 U/ml (data not shown). Even for the latter design, at Day 7 occurred an improvement in performances: V_{MAX} and LRS decreased of about 15% and 17% respectively, K_M did not undergo any substantial variation, while AA shielding suffered a worsening comparable to the one obtained for the design loading 100 U/ml (data not shown).

From these results, it is clear that enzymatic loading influences the biosensor response. As expected, at Day 1, the decreasing in enzyme loading determined a variation in kinetic and analytic parameters. In fact, as previously demonstrated [28, 29, 46], V_{MAX} reflected the amount of active enzyme molecules on the transducer surface and this parameter varied in an almost linearly manner dependently on the enzyme amount on the biosensor (data not shown, R^2= 0.951). Over time, it was observed that the presence of PG determined slight variation about LRS, while produced an interesting increase in V_{MAX}. Conversely, K_M showed different, no-predictable, trends, in fact if in

Preprints (www.preprints.org) | NOT PEER-REVIEWED | Posted: 26 October 2018 doi:10.20944/preprints201810.0630.v1

Peer-reviewed version available at Chemosensors 2018, 6, 58; doi:10.3390/chemosensors6040058

200U/ml design it decreased, in 150 U/ml design it increased and in 100 U/ml design it remained almost the same.

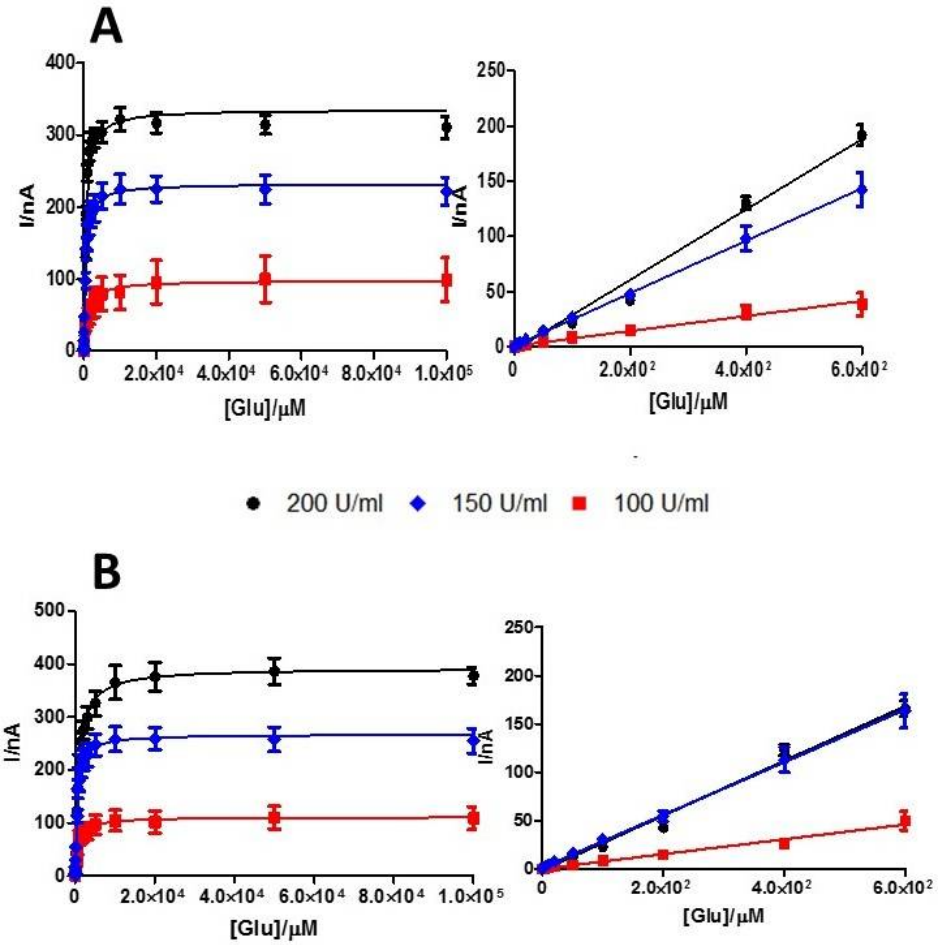

Figure 3: Michaelis-Menten kinetics plots of glutamate calibrations on different biosensor designs loading different enzyme concentrations, at Day 1 (panel A) and Day 7 (panel B), ranging from 0 to 100 mM and the relative 0-0.6 mM linear regressions. Black curve: 200 U/ml; blue curve: 150 U/ml; red curve: 100 U/ml.

3.3 Effects of the variation of propylene glycol in glutamate biosensor performances

As shown in Fig 4, the modification of propylene glycol concentration determined variations in biosensor performances, from Day 1 (Panel A) to Day 7 (Panel B). When PG was increased of ten folds, reaching 1.0% concentration (blue curve), at Day 1 a V_{MAX}= 133.32 ± 4.24 nA, a K_M= 457.90 ± 67.18 µM (R^2=0.989) and a LRS= 0.135 ± 0,003 nA/µM were obtained. If compared with 0.1 % of PG (red curve), this design demonstrated a global worsening in functioning, in fact V_{MAX} underwent a negative variation of about 65% as well as LRS, which suffered a negative change of more of 60%. Only K_M improved of about 1.3 times, showing an amelioration in substrate-enzyme affinity. The

recorded response to AA 500 µM was 1,684 ± 0,036 nA and the ΔI was 0.127 nA. The over-time performances, at Day 7, showed an overall worsening about all parameters that were 92.72 ± 4.34 nA, 854.90 ± 159.1 µM (R^2=0.992) and 0.071 ± 0.002 nA/µM respectively for V_{MAX}, K_M and LRS. AA shielding suffered a slight worsening (data not shown).

When PG was halved (black curve), that was 0.05%, the design displayed a V_{MAX}= 225.52 ± 6.23 nA, a K_M= 369.86 ± 49.60 µM (R^2=0.995) and a LRS= 0.290 ± 0,012 nA/µM. For this design, the response to AA 500 µM was 1,363 ± 0,086 nA and the ΔI was 0.221 nA. At Day 7, if compared to Day 1 performance, the global functioning of this design suffered a worsening about V_{MAX} (about -90%) and LRS (about -93%), while K_M underwent the most significant variation reaching 4091.11± 1598.01 µM, determining a substantial affinity loss of the substrate for the enzyme, also AA shielding suffered a worsening, in fact AA 500 µM gave 1,984 ± 0,079 nA and the ΔI was 0.335 nA. The global worsening of the above-mentioned design was also confirmed even if compared with the design loading PG 0.1%.

From these results it was possible to deduce that both halving and decupling enzyme concentration did not produce the best conditions for biosensor monitoring. In fact a global worsening for all parameters was observed. So, the concentration of 0.1% was chosen to study the behavior of the biosensor over a period of 21 days.

Preprints (www.preprints.org) | NOT PEER-REVIEWED | Posted: 26 October 2018 doi:10.20944/preprints201810.0630.v1

Peer-reviewed version available at Chemosensors 2018, 6, 58; doi:10.3390/chemosensors6040058

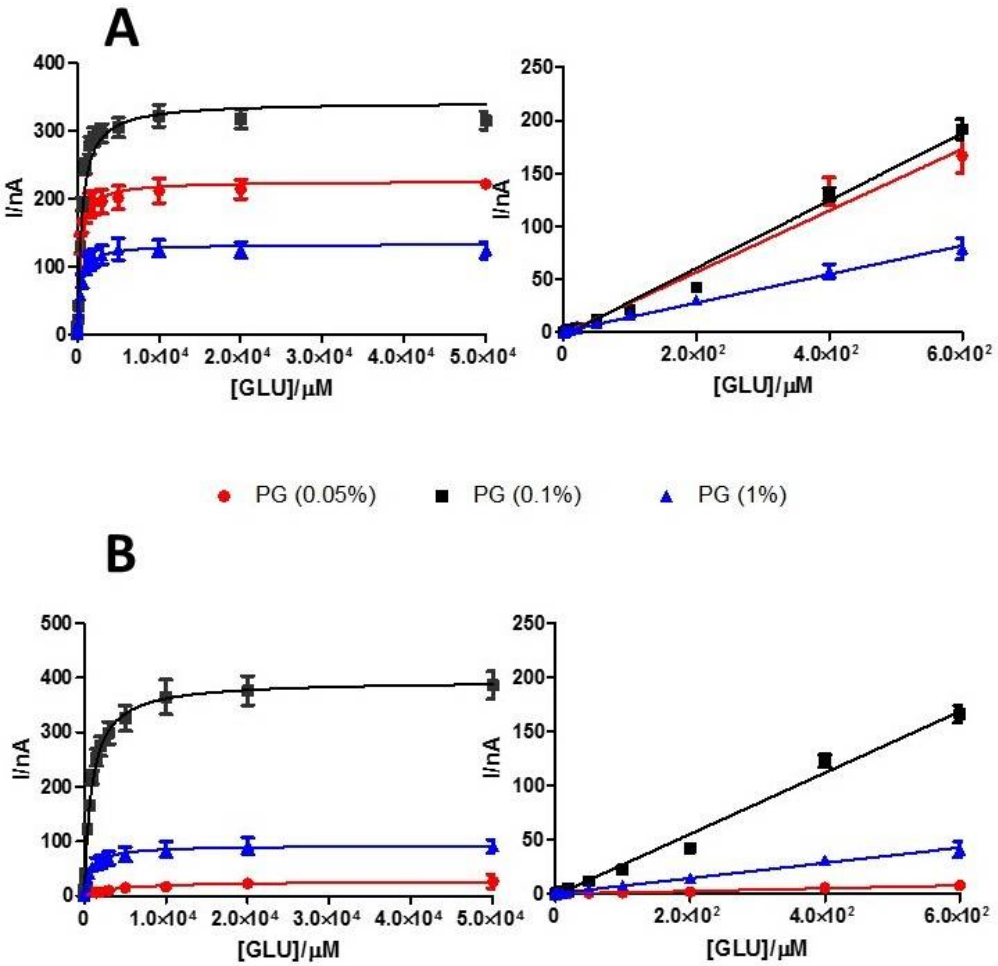

Figure 4: Michaelis-Menten kinetics plots of glutamate calibrations on different biosensor designs loading different PG concentrations, at Day 1 (panel A) and Day 7 (panel B), ranging from 0 to 100 mM and the relative 0-0.6 mM linear regressions. Black curve: PG (0.1%); blue curve: PG (1%); red curve: PG (0.05%).

3.3 Effects of PG or PEGDE on glutamate biosensor ageing

Following the interesting results, the ageing of two selected designs was evaluated. The chosen designs were the one loading PG (0.1%) and the other loading PEGDE (0.1%). As shown in Fig 5, a period of 21 days was evaluated, when for each design a full glutamate calibration was performed. As highlighted in Panel A, V_{MAX} variations of PG design (white columns) underwent a general increase up to Day 15, staring from 340.90 ± 5.92 nA at Day 1 and reaching 368.30 ± 8.11 nA at Day 15. A non-significative decrease was obtained at Day 21 when V_{MAX} reached 326.6 ± 11.14 nA.

The PEGDE design (black columns), at first showed higher values of V_{MAX}, if compared with PG design, which, after a substantial stability between Day 1 and Dy 7, showed a general decrease up to Day 21. In fact, at Day 1 and Day 7 V_{MAX} values were 409.70 ± 5.58 nA and 404.40 ± 5.26 nA

respectively. Then V_{MAX} values significantly decreased at Day 15 and day 21 until they reached 351,63 ± 5,91 nA and 310.12 ± 5,32 nA respectively, if compared with Day 1.

In Panel B, K_M over-time fluctuations are displayed. For PG design (white columns), K_M were increased similarly to V_{MAX}, between Day 1 and Day 15, ranging from K_M= 578.00 ± 40.00 µM up to K_M= 1039.00± 87.00 µM and decreasing ad Day 21 when it reached the value of 795.00 ± 116,70 µM. A significative increase of K_M was pointed out at Day 10 and Day 15, if compared with Day 1 value.

In PEGDE design (black columns), the same trend of the PG design was observed. An increase between Day 1 and Day 15 was found, ranging from K_M= 620.20 ± 37.65 µM up to K_M= 856.00 ± 91.70 µM and then a slight increase was observed at day 21 when K_M reached 879,32 ± 97,74 µM. The increases highlighted on Day 15 and Day 21 have proven to be significant when compared with the figure obtained on Day 1.

In Panel C. over-time variation of LRS are shown. In PG design, despite a slight decrease between Day 1 and Day 7, where LRS ranged from 0.323 ± 0.005 nA/µM to 0.288 ± 0.008 nA/µM, this parameter remained substantially constant up to Day 15, then, at Day 21 underwent a slight, but not significant, decrease reaching 0.253 ± 0.004 nA/µM.

In PEGDE design, it occurred a general decrease in LRS value in the considered range of time. The highest sensitivity was reached at Day 1 with a LRS=0.369 ± 0.019 nA/µM while at Day 21 a LRS=0.214 ± 0.003 nA/µM was obtained. If compared with Day 1, LRS figures from day 10 up to day 21 resulted significantly lower.

The use of PEDGE in glutamate biosensors have been widely described, its capability to stabilize enzyme molecules as well [1, 4, 35-37]. It has been shown that the cross-linking between PEGDE molecules and the enzyme is favored by the presence of the epoxide groups, whom can interact with amino groups allowing the covalent bonding of the enzyme layer to the surface [38]. In the present study, we have demonstrated that glutamate biosensors loading PEDGE (0.1%) show very good analytical performances over the period of 21 days as previously described [1], as well as the design loading PG (0.1%). Although, PEGDE showed quite interesting values in terms of V_{MAX}, K_M and LRS, PG design showed a very fascinating behavior over time. In fact, V_{MAX} values had an upward trend up to Day 15, indicating that the number of active molecules on the transducer surface was formally increased during the days. Conversely, in the PEGDE design, after a certain stability between day 1 and day 7, V_{MAX} showed a tendency to decrease over time, denoting a loss in the number of active molecules.

On the other hand, K_M behavior was, more or less, comparable between both designs. In fact, in both cases a general increase over time was achieved, as expected.

The changes in these parameters were reflected in the LRS parameter, which proved to be very interesting.

Nevertheless, although PEGDE design revealed higher values of LRS, showing a relatively-better efficiency in monitoring glutamate, but with a tendency to decrease over time, the PG design resulted in a sustained stability over a period of 15 days. In both cases, after 21 day efficiency began to change significantly.

Thus, in the present study it has been highlighted that the presence of PG it turned out to be very important for glutamate biosensor stability over time. In literature, it has been widely demonstrated the capability of molecules like propylene glycol, what polyols are, to stabilize proteins and further their long-term stability: in fact, the presence of polyols reduces the unfavorable interaction present between the solution and the proteins [47]. It has been also demonstrated that stabilizing osmolytes, as propylene glycol is, are able to move the equilibrium of proteins from denaturation to the native conformation, leading to the stabilization of the protein itself [48]. Thus, the presence of the osmolytes can change the amount of water near the protein during the reactions, determining changes also in its stability [49]. In the present study, it seems that PG has been able to interact with the proteins molecules by determining an improvement of their conformational state and producing an increase of the active molecules on the transducer surface and favoring the stability over time.

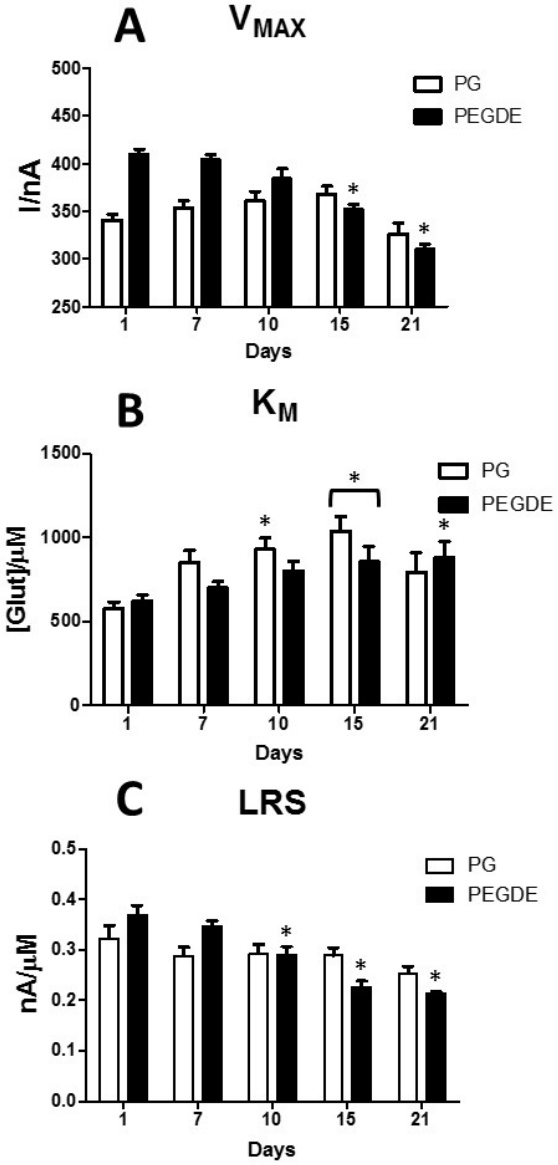

Figure 5: Bar chart describing the variations of V_{MAX} (Panel A), K_M (Panel B) and LRS (Panel C) of the two selected design Pt_c/PPD/PEI(1%)$_2$/GlutOx$_5$/PG(0.1%) (PG (0.1%)-white bars) and Pt_c/PPD/PEI(1%)$_2$/GlutOx$_5$/PEGDE(0.1%) (PEGDE (0.1%) -black bars) in the selected range of 21 days. Values are expressed as mean ± SEM. *$p<0.05$ vs Day 1.

4. Conclusions

In the present study, the role of PG has been evaluated. From results it is possible to affirm that PG helps avoiding the loss of active molecules on transducer surface but also to preserve substrate specificity, making the proposed biosensor design suitable for short- and mid-term implants in animal models.

At the moment, some experiments are underway to evaluate the role of PG on other biosensor, as glucose and lactate biosensors.

Acknowledgments:

We thank Prof. Robert D. O'Neill for inspiration regarding the glutamate biosensor. We thank him for his teachings, but, above all, for helpful and substantive discussions.

Author Contributions:

Gaia Rocchitta conceived the project, defined experimental protocol and compiled the draft; Andrea Bacciu and Paola Arrigo carried out experiments, Gianfranco Bazzu and Rossana Migheli drew plots and performed statistical analysis; Pier Andrea Serra contributed to define experimental protocol and to compile the draft.

Conflicts of Interest: The authors declare no conflict of interest.

REFERENCES

1. Ford, R.; Quinn, S.J.; O'Neill, RD. Characterization of Biosensors Based on Recombinant Glutamate Oxidase: Comparison of Crosslinking Agents in Terms of Enzyme Loading and Efficiency Parameters. Sensors (Basel) 2016, 16, pii: E1565.

2. Son, H.; Baek, J.H.; Go, B.S.; Jung, D.H.; Sontakke, S.B., Chung, H.J.; Lee, D.H.; Roh, G.S.; Kang S.S.; Cho, G.J.; Choi, W.S.; Lee, D.K.; Kim, H.J. Glutamine has antidepressive effects through increments of glutamate and glutamine levels and glutamatergic activity in the medial prefrontal cortex. *Neuropharmacology*. **2018**, *143*, 143-152.

3. Sirca, D.;Vardeu, A.; Pinna, M.; Diana, M.; Enrico, P. A robust, state-of-the-art amperometric microbiosensor for glutamate detection. Biosens Bioelectron. 2014, 61, 526-31

4. Mikeladze, E.; Collins, A.; Sukhacheva, M.; Netrusov, A.; Csöregi E. Characterization of a Glutamate Biosensor Based on a Novel Glutamate Oxidase Integrated into a Redox Hydrogel. Electroanalysis, 2002, 14, 1052-1059.

5. Burmeister, J. J.; Pomerleau, F.; Palmer, M.; Day, B.K.; Huettl, P.; Gerhardt, G. A. Improved ceramic-based multisite microelectrode for rapid measurements of L-glutamate in the CNS. J. Neurosci Meth., 2002, 119, 163-171.

6. Rieben, N.; Cherouati, N.; Martinez, K. L. Glutamate Monitoring In Vitro and In Vivo: Recent Progress in the Field of Glutamate Biosensors. Journal of Nanoneurosci. 2009, 1, 100-115.

7. Kang, Y.; Henchcliffe, C.; Verma, A.; Vallabhajosula, S.; He, B.; Kothari, P.J.; Pryor, K.O.; Mozley, P.D. 18F-FPEB PET/CT Shows mGluR5 Upregulation in Parkinson's Disease. J Neuroimaging, 2018, doi: 10.1111/jon.12563.

8. Jakaria, M.; Park, S.Y.; Haque, M.E.; Karthivashan, G.; Kim, I.S.; Ganesan, P.; Choi, D.K. Neurotoxic Agent-Induced Injury in Neurodegenerative Disease Model: Focus on Involvement of Glutamate Receptors. Front Mol Neurosci., 2018, 11, 307.

9. Müller Herde, A.; Schibli, R.; Weber, M.; Ametamey, S.M. Metabotropic glutamate receptor subtype 5 is altered in LPS-induced murine neuroinflammation model and in the brains of AD and ALS patients. Eur J Nucl Med Mol Imaging, 2018, doi: 10.1007/s00259-018-4179-9.

10. Hernandez, L.; Tucci, S.; Guzman, N.; Paez, X. In vivo monitoring of glutamate in the brain by microdialysis and capillary electrophoresis with laser-induced fluorescence detection. J Chromatogr A. 1993, 652, 393-398.

11. Globus, M.Y.; Busto, R.; Dietrich, W.D.; Martinez, E.; Valdes, I.; Ginsberg, M.D. Effect of ischemia on the in vivo release of striatal dopamine, glutamate, and gamma-aminobutyric acid studied by intracerebral microdialysis. J Neurochem. 1988, 51, 1455-1464.

12. Sheng, W.; Hang, H.W.; Ruan, D.Y. In vivo microdialysis study of the relationship between lead-induced impairment of learning and neurotransmitter changes in the hippocampus. Environ Toxicol Pharmacol. 2005, 20, 233-240.

13. Kaul, S.; Faiman, M.D.; Lunte, C.E. Determination of GABA, glutamate and carbamathione in brain microdialysis samples by capillary electrophoresis with fluorescence detection. Electrophoresis. 2011, 32, 284-291.

14. Murakami, G.; Nakamura, M.; Takita, M.; Ishida, Y.; Ueki, T.; Nakahara, D. Brain Rewarding Stimulation Reduces Extracellular Glutamate Through Glial Modulation in Medial Prefrontal Cortex of Rats. Neuropsychopharmacology. 2015, 40, 2686-2695.

15. O'Neill, R.D.; Lowry, J.P.; Rocchitta, G.; McMahon, C.P.; Serra, P.A. Designing sensitive and selective polymer/enzyme composite biosensors for brain monitoring in vivo. *Trends Anal. Chem*. **2008**, *27*, 78–88.

16. Hamdan, S.K., Mohd Zain, A. In vivo Electrochemical Biosensor for Brain Glutamate Detection: A Mini Review. *Malays J Med Sci*. **2014**, *21*, 12-26.

17. Rocchitta, G.; Spanu, A.; Babudieri, S.; Latte, G.; Madeddu, G.; Galleri, G.; Nuvoli, S.; Bagella, P.; Demartis, M.I.; Fiore, V.; et al. Enzyme biosensors for biomedical applications: Strategies for safeguarding analytical performances in biological fluids. *Sensors*. **2016**, 16, 780–800.

18. Li, Y.; Schellhorn, H.E. New developments and novel therapeutic perspectives for vitamin C. *J Nutr*. **2007**, *137*, 2171-2184.

19. Rothwell, S.A.; Kinsella, M.E.; Zain, Z.M.; Serra, P.A.; Rocchitta, G.; Lowry, J.P.; O'Neill, R.D. Contributions by a novel edge effect to the permselectivity of an electrosynthesized polymer for microbiosensor applications. *Anal Chem*. **2009**, *81*, 3911-3918.

20. Grieshaber, D.; MacKenzie, R.; Vörös, J.; Reimhult, E. Electrochemical Biosensors - Sensor Principles and Architectures. *Sensors (Basel)*. **2008**, *8*, 1400-1458.

21. Rathee, K.; Dhull, V.; Dhull, R.; Singh, S. Biosensors based on electrochemical lactate detection: A comprehensive review. *Biochem Biophys Rep*. **2015**, *5*, 35-54.

22. O'Neill, R.D.; Chang, S.C.; Lowry, J.P., McNeil, C.J. Comparisons of platinum, gold, palladium and glassy carbon as electrode materials in the design of biosensors for glutamate. *Biosens Bioelectron*. **2004**, *19*, 1521-1528.

23. McMahon, C.P.; Rocchitta, G.; Serra, P.A.; Kirwan, S.M.; Lowry, J.P.; O'Neill, R.D. The efficiency of immobilised glutamate oxidase decreases with surface enzyme loading: an electrostatic effect, and reversal by a polycation significantly enhances biosensor sensitivity. *Analyst*. **2006**, *131*, 68-72.

24. Rocchitta, G.; Secchi, O.; Alvau, M.D.; Migheli, R.; Calia, G.; Bazzu, G.; Farina, D.; Desole, M.S.; O'Neill, R.D.; Serra, P.A. Development and characterization of an implantable biosensor for telemetric monitoring of ethanol in the brain of freely moving rats. *Anal Chem*. **2012**, *84*, 7072-7079.

25. McMahon, C.P.; Rocchitta, G.; Kirwan, S.M.; Killoran, S.J.; Serra, P.A.; Lowry, J.P.; O'Neill, R.D. Oxygen tolerance of an implantable polymer/enzyme composite glutamate biosensor displaying polycation-enhanced substrate sensitivity. *Biosens Bioelectron*. **2007**, *22*, 1466-73.

26. Pisoschi, A.M. Biosensors as Bio-Based Materials in Chemical Analysis: A Review. *J Biobased Mater Bio*, **2013**, *7*, 19-38.

27. Palmisano, F.; Zambonin, P.G.; Centonze D. Amperometric biosensors based on electrosynthesised polymeric films. *Fresenius J Anal Chem* **2000**, *366*, 586–601.

28. Kirwan, S. M.; Rocchitta, G.; McMahon, C.P.; Craig, J. D.; Killoran, S.J.; O'Brien, K.B.; Serra, P.A.; Lowry, J.P.; O'Neill, R.D. modifications of poly(o-phenylenediamine) permselective layer on pt-ir for biosensor application in neurochemical monitoring. *Sensors (Basel)* **2007**, *7*, 420–437.

29. Rothwell, S.A.; Killoran, S. J.; O'Neill, R. D. Enzyme immobilization strategies and electropolymerization conditions to control sensitivity and selectivity parameters of a polymer-enzyme composite glucose biosensor. *Sensors (Basel)* **2010**, *10*, 6439–6462.

30. Cosnier, S.; Holzinger, M. Electrosynthesized polymers for biosensing. *Chem. Soc. Rev*. **2011**, *40*, 2146–2156.

31. Pal, R.K.; Pradhan, S.; Narayanan, L.; Yadavalli, V.K. Micropatterned conductive polymer biosensors on flexible PDMS films. *Sens. Actuator B-Chem*. **2018**, *259*, 498-504.

32. House, J.L.; Anderson, E.M.; Ward, W. K. Immobilization Techniques to Avoid Enzyme Loss from Oxidase-Based Biosensors: A One-Year Study. *J Diabetes Sci Technol*. **2007** Jan; *1*, 18–27.

33. El Kaoutit, M.; Naranjo-Rodriguez, I.; Dominguez, M.; Hidalgo-Hidalgo de Cisneros, J.L. Overcoming the adverse effects of crosslinking in biosensors via addition of PEG: Improved sensing of hydrogen peroxide using immobilized peroxidase. *Microchim. Acta*. **2011**, *175*, 241–250.

34. Marques, M.E.; Mansur, A.A.P.; Mansur, H.S. Chemical functionalization of surfaces for building three-dimensional engineered biosensors. *Appl. Surf. Sci.* **2013**, *275*, 347-360.

35. Burmeister, J.J.; Davis, V.A.; Quintero, J.E.; Pomerleau, F.; Huettl, P.; Gerhardt, G.A. Glutaraldehyde cross-linked glutamate oxidase coated microelectrode arrays: selectivity and resting levels of glutamate in the CNS. *ACS Chem Neurosci*. **2013**, *4*, 721-728.

36. Vasylieva, N.; Barnych, B.; Meiller, A.; Maucler, C.; Pollegioni, L.; Lin, J.S.; Barbier, D.; Marinesco, S. Covalent enzyme immobilization by poly(ethylene glycol) diglycidyl ether (PEGDE) for microelectrode biosensor preparation. *Biosens Bioelectron*. **2011**, *26*, 3993-4000.

37. Vasylieva, N.; Maucler, C.; Meiller, A.; Viscogliosi, H.; Lieutaud, T.; Barbier, D., Marinesco, S. Immobilization method to preserve enzyme specificity in biosensors: consequences for brain glutamate detection. *Anal Chem*. **2013**, *85*, 2507-2515.

38. Zigah, D.; Pellissier, M.; Fabre, B.; Barrière, F.; Hapiot, P. Covalent immobilization and SECM analysis in feedback mode of glucose oxidase on a modified oxidized silicon surface. *J. Electroanal. Chem*. **2009**, *628*, 144–147.

39. Gekko, K. Mechanism of polyol-induced protein stabilization: solubility of amino acids and diglycine in aqueous polyol solutions. *J. Biochem*, **1981**, *90*, 1633–1641.

40. Singh, S.; Singh, J. Effect of polyols on the conformational stability and biological activity of a model protein lysozyme. *AAPS PharmSciTech*. **2003**, *4*, E42.

41. Anderson, J.A. Additive effects of alcohols and polyols on thermostability of pepper leaf extracts. *J. Amer. Soc. Hort. Sci.* **2007**, *132*, 67–72.

42. Liu, F.F.; Ji, L.; Zhang, L.; Dong, X.Y.; Sun, Y. Molecular basis for polyol-induced protein stability revealed by molecular dynamics simulations. *J Chem Phys*. **2010**, *132*, 225103.

43. Yusoff, M.; Hassan, B.N.; Ikhwanuddin, M.; Sheriff, S.M.; Hashim, F.; Mustafa, S.; Koh ,I.C.C. Successful sperm cryopreservation of the brown-marbled grouper, Epinephelus fuscoguttatus using propylene glycol as cryoprotectant. *Cryobiology* **2018**, *81*, 168-173.

44. Calia, G.; Rocchitta, G.; Migheli, R.; Puggioni, G.; Spissu, Y.; Bazzu, G.; Mazzarello, V.; Lowry, J.P.; O'Neill, R.D.; Desole, M.S.; Serra, P.A. Biotelemetric monitoring of brain neurochemistry in conscious rats using microsensors and biosensors. *Sensors (Basel)*. **2009**, *9*, 2511-2523.

45. Ryan, M.R.; Lowry, J.P.; O'Neill, R.D. Biosensor for neurotransmitter L-glutamic acid designed for efficient use of L-glutamate oxidase and effective rejection of interference. *Analyst*. **1997**, *122*, 1419-1424.

46. Secchi, O.; Zinellu, M.; Spissu, Y.; Pirisinu, M.; Bazzu, G.; Migheli, R.; Desole M.S.; O'Neill, R.D.; Serra, P.A.; Rocchitta, G. Further in-vitro characterization of an implantable biosensor for ethanol monitoring in the brain. *Sensors* **2013**, *13*, 9522-9535.

47. Qarawi, M.A. Role of polyols and surfactants in liquid protein formulations. *World J Pharm Pharm Sci*. **2017**, *6*, 190-196.

48. Panuszko, A.; Bruździak, P.; Kaczkowska, E.; Stangret, J. General Mechanism of Osmolytes' Influence on Protein Stability Irrespective of the Type of Osmolyte Cosolvent. *J Phys Chem B*. **2016**, *120*, 11159-11169.

49. Timasheff, S.N. Protein-solvent preferential interactions, protein hydration, and the modulation of biochemical reactions by solvent components. *Proc Natl Acad Sci U S A* **2002**, *99*, 9721-9726.